Crimson Publishers
Wings to the Research

Mini Review

Electromagnetic Wave Scattering by a Metal Isotropic Body in a Lossless Environment with Applications to Biosciences

Panayiotis Vafeas*

Department of Chemical Engineering, University of Patras, Greece

ISSN: 2578-0247

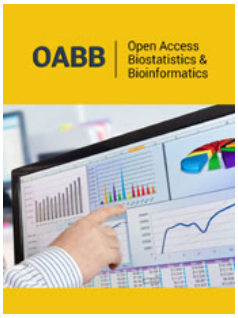

***Corresponding author:** Panayiotis Vafeas, Department of Chemical Engineering, University of Patras, 26504 Patras, Greece

Submitted: March 09, 2024

Published: April 12, 2024

Volume 3 - Issue 5

How to cite this article: Panayiotis Vafeas*. Electromagnetic Wave Scattering by a Metal Isotropic Body in a Lossless Environment with Applications to Biosciences. Open Acc Biostat Bioinform. 3(5). OABB.000572. 2024.
DOI: 10.31031/OABB.2024.03.000572

Abstract

Biomedical engineering is an interesting branch of biosciences, wherein electromagnetic wave scattering, and related fields can be applied for medical purposes. This paper investigates the electromagnetic fields, being scattered by a metal spherical object in the vacuum environment. A time-harmonic magnetic dipole source, far enough, emits at low frequencies the incident field, oriented arbitrarily in the three-dimensional space. The aim is to find a detailed solution to the scattering problem at spherical coordinates, useful for data inversion. Based on the theory of low frequencies, the Maxwell-type problem is transformed into Laplace's or Poisson's interconnected equations, accompanied by the prop-er boundary conditions on the perfectly conducting sphere and the radiation conditions at infinity, which are solved gradually. Approximating the static and the first three dynamic terms is sufficient, while the terms of higher orders are negligible.

Keywords: Biosciences; Biomedical engineering; Electromagnetic fields; Low-frequency scattering; Magnetic dipole; Spherical coordinates

Introduction

Electromagnetic waves have been extensively used in medical settings for diagnostic purposes, such as for the detection of cancerous tissues, stroke events or cardiovascular risk, as the behavior of the waves upon meeting their target gives pertinent information for diagnostic and imaging purposes. Consequently, applications related to the response of arbitrary shaped scatterers in various media, when stimulated by primary sources, stand in the frontline of the current science. Such situations are solved as electromagnetic wave scattering problems, of which there are two types. The first one concerns the forward problem, aiming to determine the scattered field via the corresponding boundary value problems of wave propagation, knowing the physical and the geometrical properties of the scatterer. The second one refers to the inverse problem, where we seek information about the nature of the scatterer, knowing its effect on the wave field. However, of greater interest is the inverse problem [1,2], which becomes particularly difficult if there is no prior knowledge of the corresponding forward problem. Hence, towards this direction, we understand the necessity to obtain efficient models, using the Maxwell's fundamental principles of electromagnetism [3] and the low-frequency scattering theory [4].

Travelling along the history, we indicatively present several references, taken from the already ample literature, which deal with mathematical wave scattering problems, whose solution show the complexity of the geometrical configuration [5] and the analytical techniques, due to the associated functions [6]. We refer to the study of the low-frequency scattering from perfectly conducting Spheres [7], Spheroids [8] and Ellipsoids [9,10], Embedded in a conductive environment and based on these analytical outcomes, an important work [11] demonstrates the efficiency of the methodology, by providing an effective solution of the inverse problem. Within this concept, more complicated geometries for the impenetrable scatteres have been investigated, like two almost touching spheres [12] or toroidal-shaped

bodies [13]. Otherwise, similar models with respect to the low-frequency scattering by metallic objects of different geometries, which are surrounded by a lossless medium [14-18], are very useful, since they find direct application to bio-medical engineering.

In this project, we intend to provide a better insight to the different structures of a solid metal scatterer in a lossless surrounding, when this body is illuminated by a magnetic dipole source that operates at low frequencies. We revisit the interesting case of the geometrically complete isotropic scatterer, as a potential application to biosciences and non-invasive medical techniques. Therein, we solve analytically the forward electromagnetic scattering problem in the low-frequency regime with the appropriately chosen conditions on the non-penetrable sphere and at infinity. Hence, we arrive to a sequence of boundary value problems, involving Laplace's and Poisson's interconnected equations, whose solution provides us with the scattered fields in terms of spherical harmonic eigenfunctions [5,6] with the proper numerical implementation.

Theoretical Development

The geometrical configuration of the scattering problem under consideration is shown in (Figure 1). In view of the Cartesian basis $(\hat{\mathbf{x}}_1, \hat{\mathbf{x}}_2, \hat{\mathbf{x}}_3)$, we define the electric field $\mathbf{E}^x$ and the magnetic field $\mathbf{H}^x$ where $x = p, s, t$ denote the primary (also referred as incident) p, the scattered s and the total t electromagnetic fields, accounting the fact that $\mathbf{E}^t(\mathbf{r}) = \mathbf{E}^p(\mathbf{r}) + \mathbf{E}^s(\mathbf{r})$ and $\mathbf{H}^t(\mathbf{r}) = \mathbf{H}^p(\mathbf{r}) + \mathbf{H}^s(\mathbf{r})$. Here, $\mathbf{r} = x_1\hat{\mathbf{x}}_1 + x_2\hat{\mathbf{x}}_2 + x_3\hat{\mathbf{x}}_3$ is the spatial position vector, while $\mathbf{r}_0$ stands for the position of the magnetic dipole $\mathbf{m}$ which radiates at a low circular frequency ω The surface S of the impenetrable ($\sigma_b \to +\infty$) spherical scatterer of radius α is characterized by the outward unit normal vector $\hat{\boldsymbol{n}}$ while the properties of the surrounding medium are the dielectric permittivity ε, the magnetic permeability μ and the electric conductivity $\sigma \to 0$ (lossless medium), being connected via the wave number $k = \omega\sqrt{\varepsilon\mu}$, in terms of the operating frequency. The area of electromagnetic scattering is confined by Ω assumed to be

$$\Omega \equiv V\left(R^3\right) - \{\mathbf{r}_0\}, \quad (1)$$

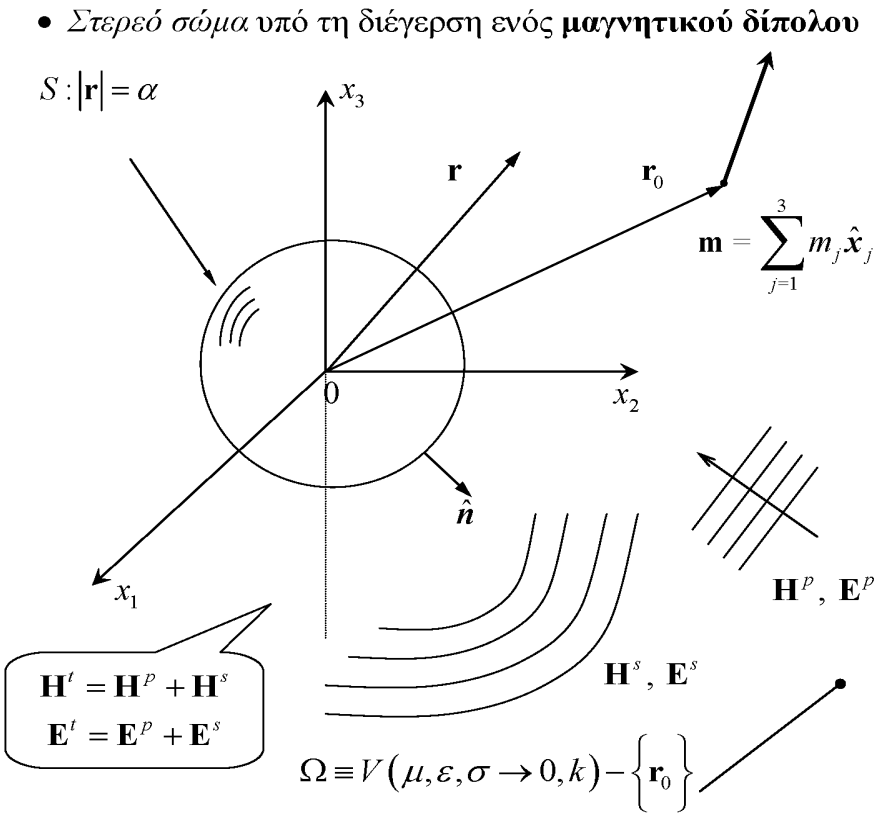

Figure 1: Representation of the scattering problem.

Excluding the singular point of the source position, whose arbitrary orientation is determined by the relation

$$\mathbf{m} = \sum_{j=1}^{3} m_j \hat{\mathbf{x}}_j. \quad (2)$$

The involved electromagnetic fields satisfy the Maxwell's equations, in view of the ∇ and Δ operators [5],

$$\nabla \times \mathbf{E}^x(\mathbf{r}) = i\omega\mu\,\mathbf{H}^x(\mathbf{r}) \text{ and } \nabla \times \mathbf{H}^s(\mathbf{r}) = -i\omega\varepsilon\,\mathbf{E}^s(\mathbf{r}) \quad (3)$$

for every $\mathbf{r} \in \Omega$ and, $x = p, s, t$, providing the Helmholtz equations.

$$\left(\Delta + k^2\right)\mathbf{E}^x(\mathbf{r}) = \left(\Delta + k^2\right)\mathbf{H}^x(\mathbf{r}) = \mathbf{0},\ \mathbf{r} \in \Omega \quad (4)$$

with boundary condition on the spherical surface

$$\hat{\boldsymbol{n}} \cdot \mathbf{H}^t(\mathbf{r}) = 0 \text{ and } \hat{\boldsymbol{n}} \times \mathbf{E}^t(\mathbf{r}) = \mathbf{0},\ \mathbf{r} \in S \quad (5)$$

for $x = p,s,t$, canceling the normal component of the total magnetic field and the tangential components of the total electric field. The radiation Silver-Müller conditions for the scattered fields are given by

$$\lim_{|\mathbf{r}|\to+\infty}\left[\mathbf{r}\times\nabla\times\begin{pmatrix}\mathbf{H}^s(\mathbf{r})\\ \mathbf{E}^s(\mathbf{r})\end{pmatrix}+ik|\mathbf{r}|\begin{pmatrix}\mathbf{H}^s(\mathbf{r})\\ \mathbf{E}^s(\mathbf{r})\end{pmatrix}\right]=\mathbf{0},\ \mathbf{r}\in\Omega, \quad (6)$$

securing the proper behavior of the fields at infinity.

Within the framework of the low-frequency theory, we expand all the fields in terms of positive integral powers of (ik), wherein i is the imaginary unit. Therefore,

$$\mathbf{H}^x(\mathbf{r})=\sum_{n=0}^{+\infty}\mathbf{H}_n^x(\mathbf{r})\frac{(ik)^n}{n!},\ \mathbf{r}\in\Omega \text{ for } x=p,s,t, \quad (7)$$

$$\mathbf{E}^x(\mathbf{r})=\sum_{n=0}^{+\infty}\mathbf{E}_n^x(\mathbf{r})\frac{(ik)^n}{n!},\ \mathbf{r}\in\Omega \text{ for } x=p,s,t. \quad (8)$$

As ω is considered very low, the term (ik) becomes low as well, thus, when $n\in\mathbb{N}$ increases, then $(ik)^n$ decreases rapidly. Therefore, without loss of generality, we restrict ourselves to orders for $n=0,1,2,3$, Since the terms of higher orders $(n\geq 4)$ can be omitted. The low-frequency expansions of the incident fields are known [14] and they imply that the surviving (non-zero) electric and magnetic scattered fields are $\mathbf{H}_0^s$, $\mathbf{H}_2^s$, $\mathbf{H}_3^s$, $\mathbf{E}_1^s$, $\mathbf{E}_3^s$ (due to the fact that $\mathbf{H}_1^p=\mathbf{E}_0^p=\mathbf{E}_2^p=\mathbf{0}$, it holds $\mathbf{H}_1^s=\mathbf{E}_0^s=\mathbf{E}_2^s=\mathbf{0}$, which are the requested scattered electromagnetic fields, which will be calculated based on the analysis that follows.

Substituting the expansions (7) and (8) into the fundamental equations (3) and the conditions (5) and (6), we arrive to a complicated sequence of boundary value problems for the scattered fields. Actually, the first task is to reduce the Maxwell's relations (3) for $x=s$ to the corresponding low-frequency counterparts, i.e.,

$$\nabla\times\mathbf{E}_n^s(\mathbf{r})=n\sqrt{\frac{\mu}{\varepsilon}}\mathbf{H}_{n-1}^s(\mathbf{r}),\ n\geq 0 \quad (9)$$

$$\text{and } \nabla\times\mathbf{H}_n^s(\mathbf{r})=-n\sqrt{\frac{\varepsilon}{\mu}}\mathbf{E}_{n-1}^s(\mathbf{r}),\ n\geq 0 \quad (10)$$

in which we have $n=0,1,2,3$. Thereafter, we are led to the interconnected partial differential equations

$$\Delta\mathbf{H}_0^s(\mathbf{r})=\mathbf{0}\ \Rightarrow\ \mathbf{H}_0^s(\mathbf{r})=\nabla\Phi_0^s(\mathbf{r}), \quad (11)$$

$$\Delta\mathbf{H}_2^s(\mathbf{r})=2\mathbf{H}_0^s(\mathbf{r})\ \Rightarrow\ \mathbf{H}_2^s(\mathbf{r})=\mathbf{X}_2^s(\mathbf{r})+\mathbf{r}\Phi_0^s(\mathbf{r}), \quad (12)$$

$$\Delta\mathbf{H}_3^s(\mathbf{r})=\mathbf{0}\ \Rightarrow\ \mathbf{H}_3^s(\mathbf{r})=\nabla\Phi_3^s(\mathbf{r}), \quad (13)$$

$$\mathbf{E}_1^s(\mathbf{r})=-\frac{1}{2}\sqrt{\frac{\mu}{\varepsilon}}\nabla\times\mathbf{H}_2^s(\mathbf{r}), \quad (14)$$

$$\Delta\mathbf{E}_3^s(\mathbf{r})=6\mathbf{E}_1^s(\mathbf{r})\ \Rightarrow\ \mathbf{E}_3^s(\mathbf{r})=\mathbf{X}_3^s(\mathbf{r})+6\left[-\frac{1}{4\pi}\iint_\Omega\frac{\mathbf{E}_1^s(\mathbf{r}')}{|\mathbf{r}-\mathbf{r}'|}d\Omega'\right], \quad (15)$$

by means of the easy-to-handle harmonic scalar Φ_0^s, Φ_3^s and vector $\mathbf{X}_2^s$, $\mathbf{X}_3^s$ functions, noting that

$$\Delta\Phi_0^s(\mathbf{r})=0,\ \Delta\mathbf{X}_2^s(\mathbf{r})=\mathbf{0},\ \Delta\Phi_3^s(\mathbf{r})=0,\ \Delta\mathbf{X}_3^s(\mathbf{r})=\mathbf{0} \quad (16)$$

for any $\mathbf{r}\in\Omega$, while the second term on the right-hand side of (15) is an immediate consequence of the fundamental solution of La-place's equation [6]. On the other hand, the surface boundary conditions (5) become.

$$\hat{\boldsymbol{n}}\cdot\mathbf{H}_n^t(\mathbf{r})\equiv\hat{\boldsymbol{n}}\cdot\left[\mathbf{H}_n^p(\mathbf{r};\mathbf{r}_0)+\mathbf{H}_n^s(\mathbf{r})\right]=0,\ n=0,2,3, \quad (16)$$

$$\hat{\boldsymbol{n}}\times\mathbf{E}_n^t(\mathbf{r})\equiv\hat{\boldsymbol{n}}\times\left[\mathbf{E}_n^p(\mathbf{r};\mathbf{r}_0)+\mathbf{E}_n^s(\mathbf{r})\right]=\mathbf{0},\ n=1,3, \quad (17)$$

whilst the infinity conditions yield

$$\lim_{|\mathbf{r}|\to+\infty}\left[\mathbf{r}\times\nabla\times\begin{pmatrix}\mathbf{H}_n^s(\mathbf{r})\\ \mathbf{E}_n^s(\mathbf{r})\end{pmatrix}+n|\mathbf{r}|\begin{pmatrix}\mathbf{H}_{n-1}^s(\mathbf{r})\\ \mathbf{E}_{n-1}^s(\mathbf{r})\end{pmatrix}\right]=\mathbf{0},\ \mathbf{r}\in\Omega. \quad (18)$$

Our goal is to solve the incorporated boundary value problems (11)-(18) by introducing the best fitted spherical geometry [5]

$$\mathbf{r}=r\zeta\hat{\boldsymbol{x}}_1+r\sqrt{1-\zeta^2}\cos\varphi\hat{\boldsymbol{x}}_2+r\sqrt{1-\zeta^2}\sin\varphi\hat{\boldsymbol{x}}_3,$$

Where $r\in[0,+\infty)$, $\zeta\equiv\cos\theta\in[-1,1]$ and $\varphi\in[0,2\pi]$ with outward unit normal vector $\hat{\boldsymbol{n}}\equiv\hat{\boldsymbol{r}}=\mathbf{r}/r$.

Spherical Scattered Fields

In order to proceed to the solution, we are obliged to present the basic mathematical tools, which are used to this project [6]. Bearing this in mind, we initially give the expansion of any harmonic function $u(\mathbf{r})$ either scalar or vector) that belongs to the kernel space of the Laplace's operator $\Delta u(\mathbf{r})=0$, that is

$$u(\mathbf{r})=\sum_{\ell=0}^{+\infty}\sum_{m=0}^{\ell}\left[A_{\ell,in}^{m/q}u_{\ell,in}^{m/q}(\mathbf{r})+A_{\ell,ex}^{m/q}u_{\ell,\text{ex}}^{m/q}(\mathbf{r})\right] \quad (19)$$

for $\mathbf{r}\in\{r\in[0,+\infty),\ \zeta\in[-1,1],\ \varphi\in[0,2\pi)\}$. Expansion (19) is a linear combination ($A_{\ell,in}^{m/q}$, $A_{\ell,ex}^{m/q}$ are arbitrary constant coefficients) with respect to the functions

$$u_{\ell,in}^{m/q}(\mathbf{r})=r^\ell Y_\ell^{m/q}(\zeta,\varphi) \quad (20)$$

$$\text{and } u_{\ell,ex}^{m/q}(\mathbf{r})=r^{-(\ell+1)}Y_\ell^{m/q}(\zeta,\varphi), \quad (21)$$

which define the respective interior and exterior spherical harmonic eigenfunctions, written in terms of the surface spherical harmonics.

$$Y_\ell^{m/q}(\zeta,\varphi)=P_\ell^m(\zeta)f_m^q(\varphi), \quad (22)$$

in view of the associated Legendre functions of the first kind $P_\ell^m(\zeta)$, where

$$f_m^q(\varphi)=\begin{cases}\cos m\varphi, & q=e\\ \sin m\varphi, & q=o\end{cases} \quad (23)$$

stand for the even $(q=e)$ and the odd $(q=o)$ trigonometric functions. The surface spherical harmonic functions $Y_\ell^{m/q}(\zeta,\varphi)$ are orthogonal with respect to the surface integral.

$$\int_0^{2\pi}\int_{-1}^{+1}Y_\ell^{m/q}(\zeta,\varphi)Y_{\ell'}^{m'/q'}(\zeta,\varphi)d\zeta d\varphi=$$

$$=\frac{1}{\varepsilon_m}\frac{4\pi}{2\ell+1}\frac{(\ell+m)!}{(\ell-m)!}\delta_{\ell\ell'}\delta_{mm'}\delta_{qq'} \quad (24)$$

for any $\ell\geq 0$, $m=0,1,2,\ldots,\ell$ and $q=e,o$. In addition, the following expansion

$$\frac{1}{R}=\frac{1}{|\mathbf{r}-\mathbf{r}_0|}=\sum_{\ell=0}^{+\infty}\sum_{m=0}^{\ell}\sum_{q=e,o}\rho_{\ell,ex}^{m/q}(\mathbf{r}_0)u_{\ell,in}^{m/q}(\mathbf{r}),\ \mathbf{r}<\mathbf{r}_0 \quad (25)$$

With

$$\rho_{\ell,ex}^{m/q}(\mathbf{r}_0)=\frac{(\ell+m)!}{(\ell+m)!}\varepsilon_m u_{\ell,ex}^{m/q}(\mathbf{r}_0) \quad (26)$$

is very useful to our calculations and refers to domains in which the singular point is far away from the scattering region $(\mathbf{r}<\mathbf{r}_0)$, as in our case.

Turning, now, to our specific problem, we remind the fact that the region of electromagnetic activity Ω is confined by the set.

$$\Omega=\left\{(r,\zeta,\varphi): r\in[\alpha,+\infty),\ \zeta\in[-1,1],\ \varphi\in[0,2\pi)\right\}-\left\{\mathbf{r}_0\right\},\ (27)$$

restricting ourselves to an exterior-type problem. Hence, the general expansion (19) is reduced accordingly to attain proper behavior at infinity, by setting $A_{\ell,in}^{m/q}=0$ herein and in every similar expansion in the forthcoming analysis. In what follows, we readily define as $\mathbf{r}_s=(r_s,\zeta,\varphi)\equiv(\alpha,\zeta,\varphi)$ and as $\mathbf{r}_0=(r_0,\zeta_0,\varphi_0)$ the position vectors pointing on the surface of the spherical body and at the position of the dipole source, while we omit to present the full analysis, since the calculations, based on (19)-(25) are cumbersome and out of the spirit of this research.

We begin with the evaluation of $\mathbf{H}_0^s$, whose solution is given through the scalar harmonic potential

$$\Phi_0^s(\mathbf{r})=-\sum_{\ell=0}^{+\infty}\sum_{m=0}^{\ell}\sum_{q=e,o}\left[\left(\frac{\mathbf{m}}{4\pi}\cdot\nabla_{\mathbf{r}_0}\rho_{\ell,ex}^{m/q}(\mathbf{r}_0)\right)\frac{\ell\alpha^{2\ell+1}}{\ell+1}r^{-(\ell+1)}Y_\ell^{m/q}(\zeta,\varphi)\right],\ (28)$$

consequently from (11), we obtain

$$\mathbf{H}_0^s(\mathbf{r})=-\sum_{\ell=0}^{+\infty}\sum_{m=0}^{\ell}\sum_{q=e,o}\left\{\frac{\ell\alpha^{2\ell+1}}{\ell+1}\frac{(\ell-m)!}{(\ell+m)!}\varepsilon_m\left[\frac{\mathbf{m}}{4\pi}\cdot\nabla_{\mathbf{r}_0}u_{\ell,ex}^{m/q}(\mathbf{r}_0)\right]\nabla u_{\ell,ex}^{m/q}(\mathbf{r})\right\},\ (29)$$

for every $\mathbf{r}\in\Omega$. Next, we proceed to the $\mathbf{H}_2^s(\mathbf{r})$, wherein we need the vector harmonic function

$$\mathbf{X}_2^s(\mathbf{r})=\sum_{\ell=0}^{\infty}\sum_{m=0}^{\ell}\sum_{q=e,o}\mathbf{b}_{\ell,ex}^{m/q}r^{-(\ell+1)}Y_\ell^{m/q}(\zeta,\varphi)\ (30)$$

and the field (27), in order to come up (via (12)) with the final expansion

$$\mathbf{H}_2^s(\mathbf{r})=\sum_{\ell=0}^{\infty}\sum_{m=0}^{\ell}\sum_{q=e,o}\left[\mathbf{b}_{\ell,ex}^{m/q}-\mathbf{r}\left(\frac{\mathbf{m}}{4\pi}\cdot\nabla_{\mathbf{r}_0}\rho_{\ell,ex}^{m/q}(\mathbf{r}_0)\right)\frac{\ell\alpha^{2\ell+1}}{\ell+1}\right]r^{-(\ell+1)}Y_\ell^{m/q}(\zeta,\varphi).\ (31)$$

The constants $\mathbf{b}_{\ell,ex}^{m/q}=b_{\ell,1}^{m/q}\hat{\mathbf{x}}_1+b_{\ell,2}^{m/q}\hat{\mathbf{x}}_2+b_{\ell,3}^{m/q}\hat{\mathbf{x}}_3$ for any value of $\ell\geq 0,\ m=0,1,2,...,\ell$ and $q=e,o,$ satisfy the three independent relationships.

$$\sum_{\ell=0}^{+\infty}\sum_{m=0}^{\ell}\sum_{q=e,o}\left[\sum_{j=1}^{3}f_{\ell,j}^{m/q,\kappa}(r_S,\zeta,\varphi)b_{\ell,j}^{m/q}-g^{m/q,r}(r_s,\zeta,\varphi;r_0)\right]=0,k=1,2,3,\ (32)$$

Wherein $f_{\ell,j}^{m/q,\kappa}(r_s,\zeta,\varphi)$ and $g_\ell^{m/q,\kappa}(r_s,\zeta,\varphi;\mathbf{r}_0)$ have complicated forms (see [14] for the exact formulae) in terms of the functions $P_\ell^m(\zeta)$, $f_m^q(\varphi)$. Thereafter, relations (32) are handled with the aid of orthogonality (24), so as to recover $\mathbf{b}_{\ell,ex}^{m/q}$. In the sequel, we move to the presentation of the solution of $\mathbf{H}_3^s$ which provides us with

$$\mathbf{H}_3^s(\mathbf{r})=\frac{1}{2\pi}\left(\frac{\alpha}{r}\right)^3\left[(2\mathbf{m}\cdot\hat{r})\hat{r}-(\mathbf{m}\cdot\hat{\boldsymbol{\zeta}})\hat{\boldsymbol{\zeta}}-(\mathbf{m}\cdot\hat{\boldsymbol{\varphi}})\hat{\boldsymbol{\varphi}}\right],\ (33)$$

Where $(\hat{r},\hat{\boldsymbol{\zeta}},\hat{\boldsymbol{\varphi}})$ denote the unit normal vectors [5] of the spherical geometry. This concludes the recovering of the magnetic low-frequency fields. Our next step includes the finding of the corresponding low-frequency electric fields, beginning with $\mathbf{E}_1^s$, so

$$\mathbf{E}_1^s(\mathbf{r})=-\frac{1}{2}\sqrt{\frac{\mu}{\varepsilon}}\sum_{\ell=0}^{\infty}\sum_{m=0}^{\ell}\sum_{q=e,o}\left\{\nabla\mu_{\ell,ex}^{m/q}(\mathbf{r})\mathrm{X}\left[\mathbf{b}_{\ell,ex}^{m/q}-\mathbf{r}\left(\frac{\mathbf{m}}{4\pi}\cdot\nabla_{\mathbf{r}_0}\rho_{\ell,ex}^{m/q}(\mathbf{r}_0)\right)\frac{\ell\alpha^{2\ell+1}}{\ell+1}\right]\right\},\ (34)$$

which is readily recovered from (31), using (14). Our final task involves the evaluation of $\mathbf{E}_3^s$, which is connected with the solution in (34), reading.

$$\mathbf{E}_3^s(\mathbf{r})=\mathbf{X}_3^s(\mathbf{r})-\frac{3}{2\pi}\iiint_\Omega\frac{\mathbf{E}_1^s(\mathbf{r}')}{|\mathbf{r}-\mathbf{r}'|}d\Omega',\ (35)$$

Where,

$$\mathbf{X}_3^s(\mathbf{r})=\sum_{\ell=0}^{\infty}\sum_{m=0}^{\ell}\sum_{q=e,o}\mathbf{d}_{\ell,ex}^{m/q}r^{-(\ell+1)}Y_\ell^{m/q}(\zeta,\varphi).\ (36)$$

At this stage, we apply a tricky mathematical technique, according to which we write.

$$-\frac{3}{2\pi}\iiint_\Omega\frac{\mathbf{E}_1^s(\mathbf{r}')}{|\mathbf{r}-\mathbf{r}'|}d\Omega'=$$

$$=\sum_{\ell=0}^{+\infty}\sum_{m=0}^{\ell}\sum_{q=e,o}\left[\boldsymbol{s}_{\ell,in}^{m/q}r^{\ell}+\mathbf{S}_\ell^{m/q}(r)+\boldsymbol{s}_{\ell,ex}^{m/q}r^{-(\ell+1)}\right]Y_\ell^{m/q}(\zeta,\varphi),\ (37)$$

Where functions $\mathbf{S}_\ell^{m/q}$, $\boldsymbol{s}_{\ell,in}^{m/q}$, $\boldsymbol{s}_{\ell,ex}^{m/q}$ are determined (e.g., see [14]) by the limiting procedure $-\frac{3}{2\pi}\iiint_\Omega\frac{\mathbf{E}_1^s(\mathbf{r}')}{|\mathbf{r}-\mathbf{r}'|}d\Omega'=$

$$=-\frac{3}{2\pi}\left\{\lim_{e\to 0}\int_0^{2\pi}\int_{-1}^{1}\int_{\alpha}^{r_0-e}\frac{\mathbf{E}_1^s(\mathbf{r}')}{|\mathbf{r}-\mathbf{r}'|}r'^2dr'd\zeta'd\varphi'+\lim_{e\to 0}\int_0^{2\pi}\int_{-1}^{1}\int_{r_0-e}^{r_0+e}\frac{\mathbf{E}_1^s(\mathbf{r}')}{|\mathbf{r}-\mathbf{r}'|}r'^2dr'd\zeta'd\varphi'+\lim_{e\to 0}\int_0^{2\pi}\int_{-1}^{1}\int_{r_0+e}^{+\infty}\frac{\mathbf{E}_1^s(\mathbf{r}')}{|\mathbf{r}-\mathbf{r}'|}r'^2dr'd\zeta'd\varphi'\right\},\ (38)$$

Therefore,

$$\mathbf{E}_3^s(\mathbf{r})=\sum_{\ell=0}^{\infty}\sum_{m=0}^{\ell}\sum_{q=e,o}\left\{\left[\left(\mathbf{d}_{\ell,ex}^{m/q}+\boldsymbol{s}_{\ell,ex}^{m/q}\right)r^{-(\ell+1)}+\boldsymbol{s}_{\ell,in}^{m/q}r^{\ell}+\mathbf{S}_\ell^{m/q}(r)\right]Y_\ell^{m/q}(\zeta,\varphi)\right\}.\ (39)$$

Again, herein, the constants $\mathbf{d}_{\ell,ex}^{m/q}=d_{\ell,1}^{m/q}\hat{\mathbf{x}}_1+d_{\ell,2}^{m/q}\hat{\mathbf{x}}_2+d_{\ell,3}^{m/q}\hat{\mathbf{x}}_3$ for any value of $\ell\geq 0,\ m=0,1,2,...,\ell$ and $q=e,o,$ satisfy the three independent expressions.

$$\sum_{\ell=0}^{+\infty}\sum_{m=0}^{\ell}\sum_{q=e,o}\left[\sum_{j=1}^{3}\overline{f}_{\ell,j}^{m/q,\kappa}(r_S,\zeta,\varphi)d_{\ell,j}^{m/q}-g_\ell^{-m/q,k}(r_s,\zeta,\varphi;r_0)\right]=0,\ \kappa=1,2,3,\ (40)$$

Wherein $\overline{f}_{\ell,j}^{m/q,\kappa}(r_S,\zeta,\varphi)$ and $\overline{g}_\ell^{m/q,\kappa}(r_S,\zeta,\varphi;\mathbf{r}_0)$ are complicated functions of ζ,φ (see [14] for the exact formulae) in terms of $P_\ell^m(\zeta)$, $f_m^q(\varphi)$. Thereafter, relations (37) are handled with the help of orthogonality (24), so as to obtain $\mathbf{d}_{\ell,ex}^{m/q}$.

Numerical Implementation

In order demonstrate the efficiency of the above analysis by means of assessing the validity and the accuracy of the produced formulae, we intend to provide plots that display the numerical

behavior of the scattered magnetic field (7) for $x = s$, i.e., $\mathbf{H}^s \equiv \mathbf{H}$ in, $\mathrm{A/m}$ which is usually measured. We approximate the low-frequency expansions up to the third degree $(n = 0,1,2,3)$ and we utilize the associated magnetic counterparts (29), (31) and (33), posing un upper limit L to the infinite series $(\ell = 0,1,...,L)$, which is appropriately chosen until convergence is obtained. We adopt the spherical geometry in Figure 1, by considering a perfectly conducting sphere of extremely large conductivity and radius $\alpha = 50\,\mathrm{m}$. The spherical body is embedded in a homogeneous vacuum environment of dielectric permittivity-ty $\varepsilon = \varepsilon_0 = 8.854\times10^{-12}\,\mathrm{F/m}$, magnetic permeability $\mu = \mu_0 = 4\pi\times10^{-7}\,\mathrm{N/A^2}$ and approximately zero electric conductivity. Thereafter, we illuminate the object with a vertically orientated dipole source $\mathbf{m} = m_3\hat{\mathbf{x}}_3$ of strength $m_3 = 4\pi\times10^3\,\mathrm{A\,m^2}$, which is set at $\mathbf{r}_0 = (200\,\mathrm{m}, 0, 200\,\mathrm{m})$ and radiates at the frequency $\omega = 50\,\mathrm{Hz}$. Bearing in mind this discussion, the scattered magnetic field $\mathbf{H}$ is evaluated along a line at $(0, 200\,\mathrm{m}, [-200, 200]\mathrm{m})$ and in (Figure 2) we provide graphical illustrations for the real and imaginary parts of the scattered magnetic field under consideration in $\mathrm{A/m}$.

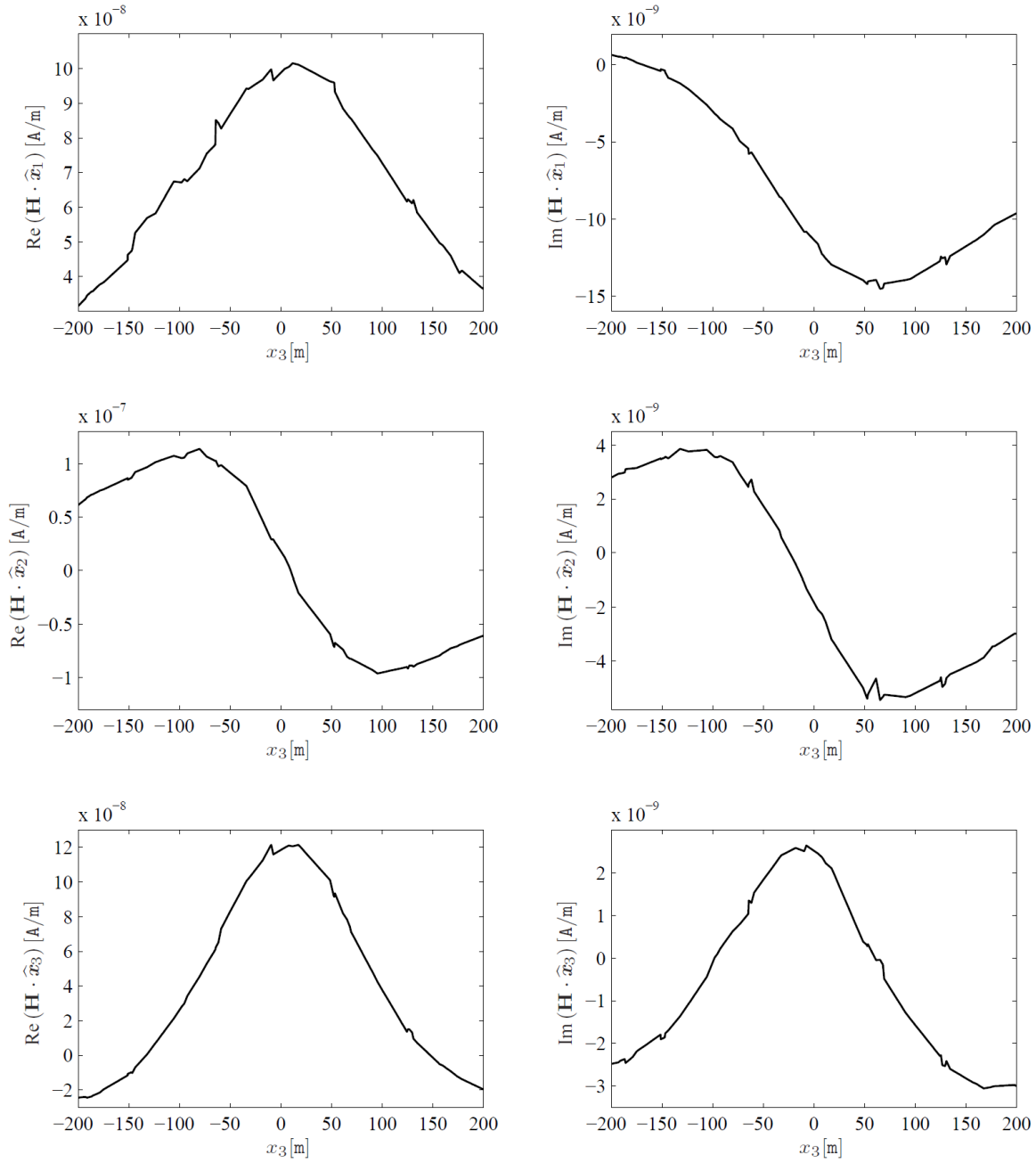

Figure 2: The real (Re) and imaginary (Im) parts of the low-frequency $(50\,\mathrm{Hz})$ scattered magnetic field in $\mathrm{A/m}$, which is excited by a vertically orientated magnetic dipole of strength $4\pi\times10^3\,\mathrm{A\,m^2}$ and location at $(200\,\mathrm{m}, 0, 200\,\mathrm{m})$. The measurement line is placed at $(0, 200\,\mathrm{m}, [-200, 200]\,\mathrm{m})$, obtaining the field on the vertical axis along x_3 in m.

The low frequency scattered magnetic field, which is sketched in (Figure 2), is verified to attain similar behavior with the respective work in the spherical realm [7], wherein the only difference is that the surrounding is conductive, changing the concept but keeping the idea. This fact secures the credibility of the obtained results in a numerical level. On the other hand, the source location and the location of the measurement line justify the set of the plotted graphs, which appear as expected. Otherwise, in an analytical level, the closed-form solutions in this project are given in a fashion that matches the procedure that is followed in many related published articles (e.g. see [14-18]) for more details.

Conclusion

In this work, we investigated the low-frequency approximation of the fields that are scattered by a perfectly conductive sphere, embedded in a lossless medium and excited by a far-field and arbitrarily orientated time-harmonic magnetic dipole, which produces the primary electric and magnetic fields. The developed analytical methodology was based on the introduction of power series expansions of the electromagnetic fields in terms of the wave number of the medium, keeping the first four terms that are sufficient in the low-frequency spectrum, while the terms of higher orders are negligible. The classical Maxwell-type problem was transformed to a sequence of interconnected elliptic-type relationships, which are accompanied by the impenetrable boundary conditions on the surface of the scatterer, while the limiting behavior at an infinite distance was readily secured. Upon the introduction of a suitable spherical geometry, the obtained boundary value problems were solved in an analytical fashion, providing three-dimensional compact formulae, in view of infinite series expansions of spherical harmonic eigenfunctions, while the outcomes of this research were validated via a consistent numerical illustration.

References

1. Ammari H, Garnier J, Jing W, Kang H, Lim M, et al. (2013) Mathematical and statistical methods for multistatic imaging Lecture Notes in Mathematics, Springer-Verlag 2098, Switzerland.
2. Ammari H, Kang H (2007) Polarization and moment tensors: with applications to inverse problems and effective medium theory. Applied Mathematical Sciences Series, Springer-Verlag, 162, New York, USA.
3. Stratton JA (1941) Electromagnetic theory. McGraw-Hill, New York, USA.
4. Dassios G, Kleinman RE (2000) Low frequency scattering. Oxford University Press, Oxford.
5. Moon P, Spencer DE (1971) Field theory handbook. Springer-Verlag, Berlin, Germany.
6. Hobson EW (1934) The theory of spherical and ellipsoidal harmonics. Monatsh f Mathematikund Physik 41: A22.
7. Vafeas P, Perrusson G, Lesselier D (2004) Low-frequency solution for a perfectly conducting sphere in a conductive medium with dipolar excitation. Progress in Electromagnetics Research 49: 87-111.
8. Vafeas P, Perrusson G, Lesselier D (2009) Low-frequency scattering from perfectly conducting spheroidal bodies in a conductive medium with magnetic dipole excitation. International Journal of Engineering Science 47(3): 372-390.
9. Perrusson G, Vafeas P, Lesselier (2010) Low-frequency dipolar excitation of a perfect ellipsoidal conductor. Quarterly of Applied Mathematics 68(3): 513-536.
10. Vafeas P (2017) Revisiting the low-frequency dipolar perturbation by an impenetrable ellipsoid in a conductive sur-rounding. Mathematical Problems in Engineering 9420658: 1-16.
11. Perrusson G, Vafeas, Chatjigeorgiou IK, Lesselier D (2015) Low-frequency on-site identification of a highly conductive body buried in Earth from a model ellipsoid. IMA Journal of Applied Mathematics 80(4): 963-980.
12. Vafeas P, Papadopoulos PK, Lesselier D (2012) Electromagnetic low-frequency dipolar excitation of two metal spheres in a conductive medium. Journal of Applied Mathematics 628261: 1-37.
13. Vafeas P, Papadopoulos PK, Ding PP, Lesselier D (2016) Mathematical and numerical analysis of low-frequency scattering from a PEC ring torus in a conductive medium. Applied Mathematical Modelling 40(13-14): 6477-6500.
14. Stefanidou E, Vafeas P, Kariotou F (2021) An analytical method of electromagnetic wave scattering by a highly conductive sphere in a lossless medium with low-frequency dipolar excitation. Mathematics 9(24): 3290.
15. Vafeas P (2018) Dipolar excitation of a perfectly electrically conducting spheroid in a lossless medium at the low-frequency regime. Advances in Mathematical Physics 9587972: 1-20.
16. Vafeas P (2020) Low-Frequency dipolar electromagnetic scattering by a solid ellipsoid in lossless environment. Studies in Applied Mathematics 145(2): 217-246.
17. Vafeas P, Lesselier D, Kariotou F (2015) Estimates for the low-frequency electromagnetic fields scattered by two adjacent metal spheres in a lossless medium. Mathematical Methods in the Applied Sciences 38(17): 4210-4237.
18. Vafeas P (2016) Low-frequency electromagnetic scattering by a metal torus in a lossless medium with magnetic dipolar illumination. Mathematical Methods in the Applied Sciences 39(14): 4268-4292.